Site-Directed Photosystem II Mutants with Perturbed Oxygen-Evolving Properties. 1. Instability or Inefficient Assembly of the Manganese Cluster *in Vivo*†

Hsiu-An Chu, Anh P. Nguyen, and Richard J. Debus*

Department of Biochemistry, University of California at Riverside, Riverside, California 92521-0129

Received November 9, 1993; Revised Manuscript Received March 14, 1994®

ABSTRACT: Several site-directed photosystem II mutants with substitutions at Asp-170 of the D1 polypeptide were characterized by noninvasive methods *in vivo*. In several mutants, including some that evolve oxygen, a significant fraction of photosystem II reaction centers are shown to lack photooxidizable Mn ions. In this fraction of reaction centers, either the high-affinity site from which Mn ions rapidly reduce the oxidized secondary electron donor, Y_Z^+, is devoid of Mn ions or the Mn ion(s) bound at this site are unable to reduce Y_Z^+. It is concluded that the Mn clusters in these mutants are unstable or are assembled inefficiently *in vivo*. Mutants were constructed in the unicellular cyanobacterium *Synechocystis* sp. PCC 6803. The *in vivo* characterization procedures employed in this study involved measuring changes in the yield of variable chlorophyll *a* fluorescence following a saturating flash or brief illumination given in the presence of the electron transfer inhibitor 3-(3,4-dichlorophenyl)-1,1-dimethylurea, or following each of a series of saturating flashes given in the absence of this inhibitor. These procedures are easily applied to mutants that evolve little or no oxygen, facilitate the characterization of mutants with labile oxygen-evolving complexes, permit photosystem II isolation efforts to be concentrated on mutants having the stablest Mn clusters, and guide systematic spectroscopic studies of isolated photosystem II particles to mutants of particular interest.

The catalytic site of photosynthetic oxygen evolution consists of a cluster of four manganese ions located in photosystem II (PSII[1]) near the lumenal surface of the thylakoid membrane. This cluster accumulates oxidizing equivalents in response to photochemical events within PSII, then oxidizes water by a mechanism that releases O_2 as a byproduct [for reviews, see Rutherford et al. (1992), Debus (1992), and Renger (1993)]. Chloride and 1–2 calcium ions are located near the manganese cluster and are required for catalysis. The photochemical events that precede water oxidation involve photoexcitation of the primary electron donor, P_{680} (a monomer or dimer of chlorophyll *a* molecules), followed by electron donation from the lowest excited singlet state of P_{680} to a nearby molecule of pheophytin *a* (Pheo). This charge separation is stabilized by the oxidation of $Pheo^-$ by a plastoquinone molecule, Q_A, and by the reduction of P_{680}^+ by a tyrosine residue, Y_Z. Further stabilization is achieved by the oxidation of Q_A^- by a second plastoquinone molecule, Q_B, and by the reduction of Y_Z^+ by the manganese cluster. The manganese cluster accumulates four oxidizing equivalents in response to four successive charge separations. The five oxidation states of the manganese cluster are termed S_n, where n denotes the number of oxidizing equivalents stored. The S_1 state predominates in dark-adapted samples. The S_4 state is a transient intermediate that spontaneously reverts to the S_0 state with the concomitant release of O_2. After accumulating two electrons in response to two successive charge separations, Q_B exchanges out of the PSII reaction center in protonated form.

The minimal oxygen-evolving PSII complex isolated to date contains at least eight subunits [for reviews, see Andersson and Styring (1991), Ikeuchi (1992), and Vermaas et al. (1993)]. Major subunits include an extrinsic 33-kDa polypeptide and the membrane-spanning proteins CP47, CP43, D1, D2, the α and β polypeptides of cytochrome *b*-559, and the product of the *psbI* gene. The photochemical events described above occur in the reaction center core of PSII. The reaction center core of PSII is a heterodimer of the D1 and D2 polypeptides.

Several lines of evidence suggest that the D1 polypeptide contributes many of the amino acid residues that coordinate the Mn and Ca^{2+} ions at the water-oxidizing site [for a review, see Debus (1992)]. This polypeptide contains numerous conserved lumenal carboxylate, histidine, and tyrosine residues (Svensson et al., 1991) that could serve as ligands to Mn or Ca^{2+} (Pecoraro, 1988; Brudvig & Crabtree, 1989). As one approach to identifying which of these residues ligate Mn or Ca^{2+}, we have employed site-directed mutagenesis to individually target each. The mutations were constructed in the unicellular cyanobacterium *Synechocystis* sp. PCC 6803. Nixon, Diner, and co-workers have employed a similar strategy and both their group and ours have published preliminary accounts in recent review articles (Diner et al., 1991; Nixon et al., 1992a; Debus, 1992). On the basis of spectroscopic studies of isolated mutant PSII particles, both groups (ours in collaboration with Barry and co-workers) have shown that Asp-170 of the D1 polypeptide is critical for the assembly or stability of the Mn cluster (Nixon & Diner, 1992; Boerner et al., 1992), serves as a component of a high-affinity binding

† This work was funded by the National Institutes of Health (GM 43496).

* Author to whom correspondence should be addressed.

® Abstract published in *Advance ACS Abstracts,* May 1, 1994.

[1] Abbreviations: bp, basepair; Chl, chlorophyll *a*; cyt, cytochrome *b*-559; DCBQ, 2,6-dichloro-*p*-benzoquinone; DCMU, 3-(3,4-dichlorophenyl)-1,1-dimethylurea; EDTA, (ethylenedinitrilo)tetraacetic acid; F_{eq}, steady-state fluorescence yield produced by weak monitoring flashes in the presence of DCMU; HEPES, *N*-(2-hydroxyethyl)piperazine-*N*′-2-ethanesulfonic acid; kb, kilobase; MES, 2-morpholinoethanesulfonic acid; P_{680}, primary chlorophyll electron donor; PCR, polymerase chain reaction; Pheo, primary pheophytin *a* electron acceptor; PSII, photosystem II; Q_A, primary plastoquinone electron acceptor; Q_B, secondary plastoquinone electron acceptor; TES, *N*-[tris(hydroxylmethyl)methyl]-2-aminoethanesulfonic acid; wild-type*, control *Synechocystis* strain constructed in the same manner as site-directed mutants, but with no mutation; Y_Z, rapid electron donor to P_{680}^+ (Tyr-161 of the D1 polypeptide); Y_D, slow electron donor to P_{680}^+ (Tyr-160 of the D2 polypeptide).

0006-2960/94/0433-6137$04.50/0

site for a Mn^{2+} ion capable of rapidly reducing Y_Z^+ (Nixon & Diner, 1992; Diner & Nixon, 1992), and may serve as a ligand to the assembled Mn cluster (Nixon & Diner, 1992; Boerner et al., 1992; Diner & Nixon, 1992). Recent work in the eukaryotic green alga *Chlamydomonas reinhardtii* confirm these findings (Whitelegge et al., 1992; J. M. Erickson, personal communication).

During our characterization of PSII particles isolated from Asp-170 mutants (Boerner et al., 1992), we observed that PSII particles from a number of other D1 mutants lost significant amounts of the extrinsic 33-kDa polypeptide and oxygen evolution during isolation (R. J. Boerner, A. P. Nguyen, B. A. Barry, and R. J. Debus, unpublished). Because the isolation procedure preserves high rates of oxygen evolution in wild-type particles (Noren et al., 1991a), these observations imply that the lability of the water-oxidizing complex is increased in some mutants. Significant losses of the 33-kDa polypeptide, manganese, and oxygen evolution have also been noted during isolation of PSII particles from the photoautotrophic Y_D-less D2 mutant, Y160F (Noren et al., 1991b; Kirilovsky et al., 1992). Increased lability of the water-oxidizing complex has also been observed in a photoautotrophic site-specific double mutant of CP47 (Putnam-Evans & Bricker, 1992).

The increased lability of the water-oxidizing complex in several PSII mutants shows that the water-oxidizing site can be significantly altered during isolation of mutant PSII particles. These isolation-induced alterations may obscure the true nature of a mutation. Determining the extent of these alterations requires characterizing mutant PSII complexes before they are isolated. Noninvasive procedures for the characterization of mutant PSII complexes *in vivo* are described in this manuscript. These procedures involve measuring changes in the yield of variable chlorophyll *a* fluorescence following a single saturating flash or brief illumination given in the presence of DCMU or following each of a series of saturating flashes given in the absence of DCMU. Such measurements are relatively easy to interpret and are easily applied to mutants that evolve little or no oxygen. The application of these procedures is illustrated by the *in vitro* characterization of several D1 mutants from which PSII particles have been isolated and characterized previously, *e.g.*, mutants at Asp-170 (Nixon & Diner, 1992; Boerner et al., 1992; Diner & Nixon, 1992). In several of these mutants, including some that evolve oxygen, a significant fraction of PSII reaction centers lack photooxidizable Mn ions *in vivo*. In this fraction of reaction centers, either the high-affinity site from which Mn ions rapidly reduce Y_Z^+ is devoid of Mn ions or the Mn ion(s) bound at this site are unable to reduce Y_Z^+. We conclude that, in these mutants, the Mn cluster is unstable or is assembled inefficiently *in vivo*.

MATERIALS AND METHODS

Growth and Preparation of Synechocystis sp. PCC 6803 Cells. *Synechocystis* cells were propagated as described by Williams (1988) at 30 °C in BG-11 media (Rippka et al., 1979). Liquid BG-11 media included 5 mM glucose (added from a separately sterilized 2 M stock solution) and 5 mM TES–NaOH (pH = 8.0). Constant illumination was provided by fluorescent cool-white bulbs at an intensity of 50–60 μE m^{-2} s^{-1} [measured with a LI-COR (Lincoln, NE) Model LI-189 light meter]. The media was held in modified 250-mL erlenmeyer flasks [similar to those described by Williams (1988)] and aerated by bubbling with sterile, humidified air. Solid media consisted of BG-11 supplemented with 1.5% (wt/v) Difco Bacto-Agar (Difco Laboratories, Detroit, MI), 10 mM TES–NaOH (pH = 8.0), 0.3% (wt/v) sodium thiosulfate, and 5 mM glucose. To eliminate selective pressure for reversion of photoautotrophically impaired or non-photoautotrophic mutants, 10 μM DCMU was included in the solid media. For selection of mutant transformants, appropriate antibiotics were also included in the solid media (see below). Antibiotics were omitted from growth media after segregation of homozygous mutants. Mutants were stored in 15% (v/v) glycerol at −80 °C (Williams, 1988).

For all assays, cells were harvested by centrifugation when their optical density at 730 nm was between 0.7 and 1.2 (measured with a Perkin-Elmer Lamda 6 UV/vis spectrophotometer). They were resuspended in growth medium at concentrations of 0.3–0.7 mg Chl/mL. The concentrated cells were placed in Eppendorf tubes on a rotating wheel under room light (12–13 μE m^{-2} s^{-1}) and aliquots were removed for analysis (we have observed that some strains lose oxygen-evolving activity if cells are left in darkness). Analyses were completed within 1–2 h of resuspending the cells. To determine the concentration of chlorophyll *a*, 10 μL of concentrated cells was mixed with 1 mL of methanol, the mixture was centrifuged, and the optical absorption spectrum of the supernatant was recorded. The concentration of chlorophyll *a* was calculated with an extinction coefficient of 79.2 $(mg/mL)^{-1}$ cm^{-1} at 665 nm (Lichtenthaler, 1987).

Isolation, PCR Amplification, and Sequencing of Synechocystis Genomic DNA. For Southern analyses, DNA was isolated from 150-mL cultures as described by Williams (1988) except that the NaI treatment was replaced by washes with 20 mM HEPES, 10 mM EDTA, pH = 7.5, and 1.5 M KCl, 5 mM EDTA, pH = 7.5 (suggested by B. A. Barry). For PCR amplification, DNA was isolated from a pea-sized glob of cells as described by Chisholm (1989). The oligonucleotides 5′-CCAAAACGCCCTCTGTTTACC-3′ and 5′TCGATGGCAATCAAGATCAGC-3′ were employed for PCR amplification of a 1380-bp fragment containing the entire *psb*A-2 gene of *Synechocystis* sp. PCC 6803. These oligonucleotides hybridize to complementary DNA strands approximately 180 bp upstream and 110 bp downstream of *psb*A-2, respectively. Amplification involved 25 cycles of 1 min at 94 °C, 1 min at 55 °C, and 2 min at 72 °C in the reaction mixture recommended by Perkin-Elmer Cetus (Norwalk, CT). The amplified mixture was extracted with phenol and chloroform, precipitated with ethanol, and then suspended in 25 μL of 10 mM Tris-HCl, 1 mM EDTA, 100 mM NaCl, pH = 8. Primers were removed by centrifugation through 1 mL of Sepharose CL-6B (Pharmacia LKB Biotechnology, Piscataway, NJ) packed in a 1.5-mL column reservoir in the same buffer (DuBoise & Hartl, 1990). For DNA sequencing, *psb*A-2 primers were annealed with the double-stranded 1380-bp PCR products by heating at 95 °C for 2 min and then freezing in dry ice/ethanol for 5 min (Kusukawa et al., 1990; P. J. Nixon, personal communication). Sequences were obtained with T7 DNA polymerase.

Construction and Verification of Site-Directed Mutants. All mutants were constructed in the *psb*A-2 gene of *Synechocystis* sp. PCC 6803. Construction of the mutants D170E, D170N, and D170A was described previously (Boerner et al., 1992). Other mutants were constructed as described previously (Debus et al., 1988) and were introduced (Williams, 1988) into a strain of *Synechocystis* sp. PCC 6803 that lacks all three of its *psb*A genes (Debus et al., 1990). The wild-type* strain was obtained by identical procedures, except that the transforming plasmid carried no mutation. Mutants were selected on solid media containing the antibiotics kanamycin

monosulfate (5 μg/mL), spectinomycin dihydrochloride (20 μg/mL), and chloramphenicol (2.5 μg/mL) (Debus et al., 1990). To confirm that homologous recombination had taken place, genomic DNA was isolated from each mutant, digested with *Xba*I, and analyzed by Southern blots (Debus et al., 1990). To confirm the identity of each mutant and to verify the absence of undesired mutations, the complete sequence of *psb*A-2 was obtained by direct sequencing of the 1380-bp double-stranded PCR product described above. To verify that no mutations outside the *psb*A-2 coding region contribute to the loss of photoautotrophy in non-photoautotrophic mutants, cells of these mutants were transformed with a cloned fragment of the wild-type *psb*A-2 gene that included the desired mutation site. In every case, photoautotrophic transformants were recovered at frequencies that were far higher than the frequency at which spontaneous photoautotrophic revertants appeared. Virtually all mutants were constructed with a "silent" mutation close to the desired mutation site. These silent mutations introduced or removed convenient sites for restriction endonucleases. To verify that the silent mutations do not contribute to loss of photoautotrophy, spontaneous photoautotrophic revertants of non-photoautotrophic mutants were isolated and their *psb*A-2 genes amplified by PCR and sequenced. In every case in which the desired mutation had been created with a single base change, the desired mutation had reverted (or a codon synonymous with the wild-type codon had been generated), but the silent mutation remained.

Measurement of Photosynthetic Oxygen Evolution. Concentrated cells were diluted into growth medium held at 25.0 °C in a stirred, stoppered, water-jacketed cell (Gilson Medical Electronics, Middleton, WI). Potassium ferricyanide (2 mM) and 2,6-dichloro-*p*-benzoquinone (2 mM) were added to the medium immediately prior to the addition of the cells. The volume of the final solution was 1.6 mL and contained 32 μg chlorophyll and 2% ethanol. The 2,6-dichloro-*p*-benzoquinone (Eastman Kodak Laboratory Chemicals, Rochester, NY) was purified by recrystallization from methanol or by sublimation. The water-jacketed cell was fitted with a YSI (Yellow Springs Instrument Co., Yellow Springs, OH) Model 5331 Clark-type oxygen electrode. Saturating illumination was provided by a Dolan-Jenner (Woburn, MA) Model 180 fiber optics illuminator equipped with an EJV bulb. The light was passed through Dolan-Jenner infrared and red cuttoff filters and directed to one side of the cell with a 0.5 in. active diameter Dolan-Jenner fiber optic light guide. A front-surface mirror was attached to the opposite side of the cell. The zero level of light-saturated oxygen evolution was established with the *Synechocystis* strain that lacks all three *psb*A genes (Debus et al., 1990). Under our assay conditions, this strain exhibits an *apparent* oxygen evolution rate of 16 ± 7 μmol O_2 (mg of Chl)$^{-1}$ h^{-1} (29 cultures examined). The origin of this background activity is unknown but is presumably artifactual. The oxygen evolution rates of all other strains were corrected by subtracting this background. The corrected light-saturated oxygen-evolution rate exhibited by the eight wild-type* cultures examined in this study was 680 ± 30 μmol O_2 (mg of Chl)$^{-1}$ h^{-1}.

Measurement of Chlorophyll a Fluorescence. Chlorophyll *a* fluorescence was detected with a Walz (Effeltrich, Germany) pulse-amplitude-modulation fluorometer [described by Schreiber (1986)]. Weak monitoring flashes (λ = 650 nm) of 1-μs duration were applied at 1.6 kHz or 100 kHz, as noted. The fluorometer was modified with the help of the manufacturer so that (i) the amplifier gating time could be varied, (ii) actinic flashes could be triggered at rates up to at least 20 Hz, and (iii) the time during which the monitoring flashes can be automatically applied at 100 kHz could be decreased to 1 ms. For most experiments, the amplified output of the fluorometer was recorded with a Zenith AT computer via the Walz DA-100 data-acquisition system. For experiments involving measuring the fluorescence yield after each flash in a series, the amplified output was recorded with a LeCroy (Chestnut Ridge, NY) Model 9310M digital oscilloscope. When DCMU was present, single saturating flashes (ca. 11 μs width at half-maximum) were provided by a Walz XST-103 xenon flash lamp, which incorporates a 2 mm thick Schott BG-11 blue-green filter at its exit. When DMCU was absent, saturating flashes (ca. 2.5 μs at half-maximum) were provided by an EG&G (Salem, MA) Model FX-193 xenon flash lamp and were passed through a 2 mm thick Corning/Kopp CS 4-96 blue filter. The fluorometer's photodiode detector is protected by a 1 mm thick Schott RG-9 red filter. To prevent saturation of the photodiode amplifier, the amplifier was gated for 75 μs when each actinic flash was triggered. Because the amplifier requires time to restabilize, data acquisition was interrupted for a total of approximately 105 μs when each flash was triggered. Continuous illumination was provided by a Schott (Southbridge, MA) Model KL-1500 fiber optics illuminator and was passed through a heat filter and a Balzers DT Cyan short-pass filter (λ < 680 nm). The light intensity at the sample was 800 μE m^{-2} s^{-1}. Illumination was controlled by a Uniblitz Model VS14 shutter operated by a Model T-132 shutter driver (Vincent Associates, Rochester, NY). The shutter opened in 1.5 ms and closed in 3.0 ms. The illuminator and shutter were connected with an 8 mm active diameter Schott flexible light guide. The sample was contained in a water-jacketed cuvette (Walz KS-101) having a reflective bottom and containing a flea-type stirring bar. The sample cuvette was connected to the fluorometer and light sources by a four-arm fiber optics light guide (Walz 101-F).

For measurements, concentrated cells were diluted into a solution of 50 mM MES–NaOH, 25 mM $CaCl_2$, 10 mM NaCl, pH = 6.5, held in the sample cuvette at 22 °C. The volume of the final solution was 0.58 mL and contained 20 μg of chlorophyll. For measurements of the fluorescence yield after each flash in a series, samples were incubated in darkness for 1 min before the weak monitoring flashes were switched on. The saturating actinic flashes were applied approximately 1 min later. For measurements of Q_A^- charge recombination kinetics after a flash or continuous illumination, samples were incubated in darkness for 1 min in the presence of 0.3 mM *p*-benzoquinone (purified by sublimation) and 1 mM potassium ferricyanide. DCMU was then added to a concentration of 40 μM (the final concentration of ethanol was 2%) and the weak monitoring flashes were switched on. In response to these flashes, the fluorescence rose from an initial level of F_0 to a steady state level which we denote "F_{eq}". The ratio $(F_{eq} - F_0)/(F_{max} - F_0)$ ranged from ca. 0.25 in the wild-type* and D170E mutants to ca. 0.11 in the D170H and D170R mutants and to ca. 0.05 in the D170N, D170A, and D170T mutants. Actinic illumination was applied ca. 3 min after the monitoring flashes were switched on, after a stable F_{eq} level had been achieved. The short dark-adaptation periods were chosen because some mutants were found to lose oxygen-evolving activity rapidly in darkness. The kinetics of Q_A^- oxidation were analyzed using Jandel Scientific's (San Rafael, CA) PeakFit program, version 3.18.

To measure the total yield of variable chlorophyll *a* fluorescence ($F_{max} - F_0$) samples were incubated in darkness with *p*-benzoquinone and ferricyanide as above, but for 5 min

to allow for the full oxidation of Q_B^- (Wollman, 1978). DCMU was then added as above, followed 1 min later by hydroxylamine to a concentration of 20 mM (from a fresh 0.5 M solution of hydroxylamine hydrochloride adjusted to pH = 6.5 with NaOH). The weak monitoring flashes were switched on 20 s after the addition of hydroxylamine, followed 1 s later by continuous actinic illumination. The difference between the maximum fluorescence produced by the actinic illumination (F_{max}) and the initial fluorescence measured by the monitoring flashes (F_0) was used as a relative measure of the PSII content in samples containing the same concentration of Chl.

Measurement of [^{14}C]DCMU Binding. The quantitation of PSII on a chlorophyll basis was performed as described previously (Boerner et al., 1992) on the basis of methods developed by Vermaas and co-workers (Vermaas et al., 1990). Cells (25 μg of chlorophyll diluted to 1 mL with growth medium) were incubated for 30–60 min in darkness in the presence of 20–300 nM [^{14}C]DCMU [243 μCi/mg; Amersham, kindly supplied by W. F. J. Vermaas (Arizona State University)]. To control for nonspecific or non-PSII binding of DCMU, duplicate samples were incubated in the presence of 20 μM atrazine. All samples contained 0.6% methanol. After incubation, samples were centrifuged, and 0.8 mL of each supernatant was removed for scintillation counting. For each concentration of DCMU, the concentration of bound DCMU was determined by subtracting the concentration of free DCMU in samples without atrazine from the concentration in samples with atrazine. The concentration of specifically bound DCMU at saturation and the K_D of the reaction centers for DCMU were estimated from direct linear plots (Eisenthal & Cornish-Bowden, 1974; Cornish-Bowden, 1979). In a conventional double-reciprocal plot [*e.g.*, see Vermaas et al. (1990)], each pair of $[DCMU]_{free}$ and $[DCMU]_{bound}$ values is represented by a point. In a direct linear plot, each pair of $[DCMU]_{free}$ and $[DCMU]_{bound}$ values is represented by a line with intercept $-[DCMU]_{free}$ on the horizontal axis and intercept $[DMCU]_{bound}$ on the vertical axis. An example of such a plot is given in Figure 1. In this figure, the eight pairs of $[DCMU]_{free}$ and $[DCMU]_{bound}$ values are represented by eight lines. In the absence of experimental error, all lines on a direct linear plot intersect at a common point whose ordinate corresponds to the $[DCMU]_{bound}$ at saturation and whose abscissa corresponds to the K_D of the reaction centers for DCMU. In the presence of experimental error, for n lines there are $^1/_2n(n-1)$ intersection points. The best estimate of the true $[DCMU]_{bound}$ at saturation is the median of the $^1/_2n(n-1)$ ordinate values, while the best estimate of K_D is the median of the $^1/_2n(n-1)$ abscissa values. The precision of these estimates is readily estimated from the spread in the $^1/_2n(n-1)$ ordinate and abscissa values (Porter & Trager, 1977). The advantages of the direct linear plot over the double-reciprocal plot are (i) accurate estimates of $[DCMU]_{bound}$ at saturation and K_D do not require the use of the *weighted* least squares analysis that is required to overcome the distortions inherent in plotting data in double-reciprocal form and (ii) aberrant data have little affect on the estimated parameters because they are determined from the median abscissa and ordinate values of the intersection points, rather than from their means.

RESULTS

Growth and Oxygen-Evolution Characteristics of Mutant Cells. The growth characteristics and light-saturated oxygen-evolution rates of the mutant strains described in this manuscript are listed in Table 1. In addition to the Asp-170 mutants, this table lists three other mutants (E65A, D342E, and Δ*psb*O) that are mentioned briefly in this paper to illustrate particular points. The Δ*psb*O strain lacks the *psb*O gene, which encodes the extrinsic 33-kDa polypeptide. This strain was kindly provided by R. L. Burnap (Oklahoma State University) and was described previously (Burnap & Sherman, 1991). The data in Table 1 agree with previous characterizations of Asp-170 mutants (Nixon & Diner, 1992; Boerner et al., 1992) and mutants that lack a functional *psb*O gene [*e.g.*, see the work of Burnap and Sherman (1991), Philbrick et al. (1991), and Mayes et al. (1991)]. As previously described (Nixon & Diner, 1991; Boerner et al., 1992), cultures of the D170E and D170H mutants grew photoautotrophically, the former at the same rate as wild-type* cells, the latter at a diminished rate. Both mutants evolved oxygen at ca. 50% the rate of wild-type* cells. The other Asp-170 mutants (D170R, D170N, D170A, and D170T) were obligate photoheterotrophs, requiring 5 mM glucose for propagation. Cultures of the D170R and D170N mutants evolved oxygen at low rates (ca. 12% and 5%, respectively) compared to wild-type* cells. Because some mutants (*e.g.*, D170N) have nonnegligible rates of spontaneous reversion, we sought to determine if the low rates of oxygen evolution observed in the D170R and D170N cultures arose from populations of reverted cells. Therefore, we spread duplicate serial dilutions of oxygen-evolving D170R and D170N cultures on solid media containing and lacking glucose. The examined cultures contained fewer than one revertant in 10^4 cells (data not shown). These results demonstrate that the oxygen-evolution rates observed in the D170R and D170N cultures were intrinsic to these mutants. Cultures of the E65A, D342E and Δ*psb*O mutants grew photoautotrophically, but at diminished rates. The E65A and D342E mutants evolved oxygen at approximately 20% the rate of wild-type* cells, while the Δ*psb*O mutant evolved oxygen at 34 ± 3% the rate of wild-type* cells. In darkness, the oxygen-evolution activity of concentrated Δ*psb*O cells de-

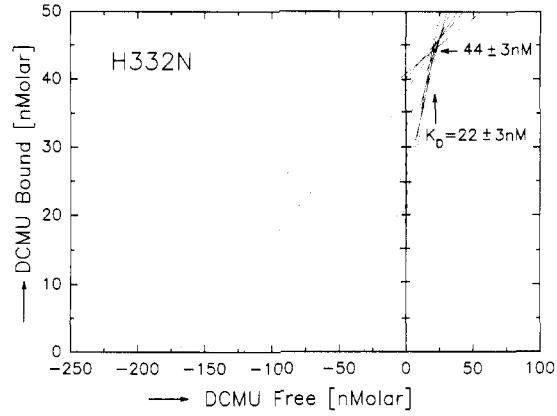

FIGURE 1: Direct linear plant for determining the amount of [^{14}C]-DCMU specifically bound to PSII reaction centers in H332N cells at saturation and for determining the K_D of these reaction centers for DCMU. Eight aliquots of cells (25 μg/mL chlorophyll) were incubated in the presence of 20–300 nM [^{14}C]DCMU and 0.6% methanol. The eight pairs of $[DCMU]_{free}$ and $[DCMU]_{bound}$ values obtained from these aliquots were, in nanomolar, (246, 40.8), (171, 40.0), (121, 38.0), (64.1, 33.0), (39.2, 28.1), (31.4, 25.4), (19.8, 22.2), and (17.4, 20.1). Each of these eight pairs of points defines a line with intercept $-[DCMU]_{free}$ on the horizontal axis and $[DCMU]_{bound}$ on the vertical axis. From the position and spread of the intersection points of these eight lines, one may determine that, at saturating concentrations of DCMU, 44 ± 3 pmol of DCMU binds to 25 μg of Chl in 1 mL with a K_D of 22 ± 3 nM. The former value corresponds to one DCMU site per 640 ± 40 chlorophyll *a* molecules. For details of the experimental procedures, see Materials and Methods.

Table 1: Comparison of Wild-Type* (wt*) and Mutant Strains Whose Kinetics of Q_A^- Oxidation Are Discussed

strain	photoautotrophic growth[a]	O_2 evolution[b] (% of wt*)	PSII content[c] (% of wt*)	kinetics of Q_A^- oxidation[d] after a single flash[e] (%)	after a single flash[e] k^{-1} (s)	after 5 s of illumination[f] (%)	after 5 s of illumination[f] k^{-1} (s)	no. cultures included in analyses
wild-type*	+	100	100	16 ± 4	0.10 ± 0.04	56 ± 7	0.53 ± 0.07	
				43 ± 4	0.60 ± 0.13	36 ± 6	3.0 ± 0.5	8
				41 ± 7	2.8 ± 0.4	7.2 ± 0.9	60 ± 18	
D170E	+	55 ± 5	92 ± 17	29 ± 6	0.076 ± 0.033	48 ± 4	0.26 ± 0.01	
				43 ± 4	0.36 ± 0.06	31 ± 4	2.8 ± 0.3	4
				28 ± 4	3.7 ± 0.3	20 ± 0.4	80 ± 20	
D170H	+ (slow)	46 ± 11	92 ± 18	34 ± 6	0.049 ± 0.006	37 ± 6	0.41 ± 0.17	
				36 ± 2	0.50 ± 0.12	26 ± 7	2.4 ± 0.7	4
				29 ± 6	2.6 ± 0.2	36 ± 0.5	175 ± 90	
D170R	–	12 ± 2	95 ± 11	51 ± 6	0.050 ± 0.017	27 ± 4	0.48 ± 0.15	
				29 ± 3	0.83 ± 0.26	28 ± 4	3.6 ± 0.4	4
				19 ± 4	7.3 ± 1.9	44 ± 3	130 ± 90	
D170N	–	5 ± 2	130 ± 24	49 ± 5	0.015 ± 0.005	44 ± 4	0.13 ± 0.02	
				43 ± 5	0.12 ± 0.04	11 ± 3	5.4 ± 2.0	4
				7.6 ± 1.5	3.4 ± 1.1	46 ± 1	75 ± 30	
D170A	–	0	135 ± 24	53 ± 18	0.0035 ± 0.0029	22 ± 5	0.054 ± 0.014	
				43 ± 18	0.017 ± 0.009	5.9 ± 1.3	3.8 ± 1.2	10
				3.7 ± 2.4	0.52 ± 0.41	72 ± 6	135 ± 60	
D170T	–	0	99 ± 12	67 ± 6	0.033 ± 0.008	38 ● 4	0.18 ± 0.02	
				25 ± 4	0.27 ± 0.06	10 ± 1	3.0 ± 0.7	7
				6.9 ± 1.1	4.1 ± 1.3	52 ± 3	150 ± 80	
E65A	+ (slow)	20 ± 5	89 ± 17	32 ± 12	0.050 ± 0.035	63 ± 4	0.23 ± 0.02	
				54 ± 6	0.26 ± 0.12	9 ± 2	3.9 ± 0.7	4
				14 ± 8	3.3 ± 2.4	28 ± 3	86 ± 14	
D342E	+ (slow)	18 ± 3	85 ± 17	25 ● 7	0.034 ± 0.018	65 ± 2	0.28 ± 0.01	
				58 ± 6	0.26 ± 0.11	10 ± 2	4.3 ± 1.3	4
				17 ± 9	3.7 ± 2.5	24 ± 4	105 ± 45	
Δ*psb*0	+	34 ± 3	72 ± 12	20 ± 4	0.14 ± 0.03	45 ± 7	1.2 ± 0.2	
				33 ± 7	1.2 ± 0.3	46 ± 5	9.1 ± 1.3	4
				48 ± 5	8.1 ± 0.8	9 ± 4	100 ± 50	

[a] Measured in growth medium without glucose. [b] The eight wild-type* cultures used in this study exhibited 680 ± 30 μmol O_2 (mg of Chl)$^{-1}$ h^{-1}. [c] Estimated from the total yield of variable chlorophyll *a* fluorescence ($F_{max} - F_0$). [d] Measured in the presence of DCMU and analyzed assuming three exponentially decaying components. The relative amplitude (%) and the inverse of the rate contant of each component are reported. [e] See Figures 2 and 7. [f] See Figure 5.

creased by 60–80% with a halftime of 8–12 min (not shown).

Quantitation of Photosystem II Reaction Centers in Mutant Cells. The total yield of variable chlorophyll *a* fluorescence ($F_{max} - F_0$) has been used as a measure of the relative PSII content of cyanobacterial cells (Philbrick et al., 1991; Nixon & Diner, 1992; Nixon et al., 1992b). The basis for this assay is that the fluorescence yield of cyanobacteria and chloroplasts arises primarily from PSII and is governed by the redox states of Q_A (Duysens & Sweers, 1963) and P_{680} (Butler, 1972; Butler et al., 1973) [for reviews, see Holzwarth (1991), Krause & Weis (1991), and Holzwarth & Roelofs (1992)]. When Q_A is fully oxidized (achieved by incubating cells in darkness with *p*-benzoquinone and ferricyanide) the fluorescence yield (F_0) is low. When Q_A is fully reduced (achieved by illuminating cells in the presence of DCMU and an exogenous electron donor such as hydroxylamine) the fluorescence yield (F_{max}) is 2–5-fold greater than F_0. This increase comes about because the rate constant of charge separation decreases when Q_A is reduced (Schatz et al., 1988; Leibl et al., 1989; Roelofs et al., 1992), presumably because of the electrostatic influence of Q_A^- on $Pheo^-$ (Schatz et al., 1988). The diminished rate constant decreases the yield of charge separation, thereby increasing the lifetime of the excited state of the antenna chlorophylls, from which the fluorescence emanates.

Determining the total yield of variable chlorophyll fluorescence is a simple and rapid method for quantifying PSII and requires little material. The method's accuracy has been checked for some cultures by comparison with detergent-extracted PSII core complexes (Philbrick et al., 1991). Nevertheless, in some mutants, mutation-induced structural changes might alter the rate constant of charge separation and its dependence on the redox state of Q_A. Under such circumstances, mutants with the same PSII content might exhibit different total yields of variable chlorophyll fluorescence. Consequently, the total yield of variable chlorophyll fluorescence may not accurately reflect the relative PSII content of mutants. An alternate method for quantifying PSII in cyanobacterial cells is to measure the specific binding of [^{14}C]DMCU [*e.g.*, see Vermaas et al. (1990)]. This method also reveals the structural integrity of the Q_B site by providing its K_D for DCMU.

To determine if the total yield of variable chlorophyll fluorescence accurately reflects the PSII content of mutant cells, we performed both [^{14}C]DMCU binding and variable fluorescence measurements on cells of 21 different mutants. For each mutant, both methods were performed on the same culture. Table 2 shows the relative PSII contents determined by each method. Table 2 also lists the ratio of chlorophyll to PSII in each culture determined by [^{14}C]DMCU binding (assuming one atrazine-sensitive DCMU site per PSII) and the K_D for DCMU binding. Taking into account the precision of the estimates, the data show that the total yield of variable chlorophyll fluorescence ($F_{max} - F_0$) provides a reasonably accurate estimate of the relative PSII content of mutant cells, even in mutants whose PSII content differs considerably from that of wild-type* cells. Indeed, the relative PSII contents determined by the two methods are related by a linear correlation coefficient of 0.94, showing a very high degree of correlation.

The correspondence between the total yield of variable chlorophyll fluorescence and PSII content shown in Table 2 implies that the rate constant of charge separation and its

Table 2: Comparison of the Relative PSII Contents of Wild-Type* and Mutant Strains Determined from [^{14}C]DCMU Binding and from Chlorophyll *a* Fluorescence Measurements

	from [^{14}C]DCMU binding[a]			from chlorophyll fluorescence[b]
strain	Chl/DCMU	K_D (nM)	PSII content (% of wild-type*)	PSII content (% of wild-type*)
wild-type*	470 ± 60	12 ± 2	100	100
D61E	370 ± 20	18 ± 2	125 ± 16	91 ± 11
D61N	650 ± 50	16 ± 3	72 ± 10	81 ± 9
D61A	700 ± 50	15 ± 3	67 ± 10	76 ± 9
E65D	510 ± 30	12 ± 2	92 ± 12	86 ± 10
E65Q	490 ± 30	16 ± 2	95 ± 13	95 ± 11
E65A	510 ± 20	17 ± 3	92 ± 12	87 ± 10
D170E	630 ± 20	11 ± 1	74 ± 9	82 ± 9
D170N	520 ± 15	15 ± 1	90 ± 11	102 ± 12
D170A	330 ± 30	26 ± 3	140 ± 20	150 ± 17
E189D	410 ± 30	23 ± 3	114 ± 16	101 ± 12
E189Q	400 ± 20	16 ± 4	117 ± 15	105 ± 12
H332Q	530 ± 20	16 ± 3	88 ± 11	79 ± 9
H332N	640 ± 40	23 ± 3	73 ± 10	65 ± 7
H332L	1640 ± 200	23 ± 3	28 ± 5	20 ± 2
E333D	1650 ± 150	22 ± 7	28 ± 4	29 ± 3
E333Q	590 ± 40	13 ± 4	79 ± 11	83 ± 10
H337Q	680 ± 30	17 ± 4	69 ± 9	68 ± 8
H337L	840 ± 50	17 ± 3	56 ± 8	66 ± 8
D342E	480 ± 40	15 ± 2	98 ± 15	97 ± 11
D342N	1100 ± 90	23 ± 3	42 ± 6	43 ± 5
D342A	3200 ± 300	22 ± 6	15 ± 2	22 ± 3

[a] Estimated from direct linear plots (see Figure 1 and text). [b] Estimated from the total yield of variable chlorophyll *a* fluorescence ($F_{max} - F_0$). The ratio $(F_{max} - F_0)/F_0$ was 0.79 ± 0.04 for the seven wild-type* cultures examined.

dependence on the redox state of Q_A are largely unaffected in all 21 mutants, suggesting that the PSII complexes in these mutants are relatively intact. In support of this suggestion, no mutant exhibited a K_D for DCMU that was more than 2-fold greater than for wild-type* cells. Because of the correspondence between the two methods, the relative PSII contents of mutant cultures were routinely determined by measuring their total yields of variable chlorophyll fluorescence. Table 1 lists the relative PSII contents of the mutant strains discussed in this paper. For each entry, 4–10 separate cultures were analyzed. All mutants except Δ*psb*O contained at least 85% the PSII content of wild-type* cells. The Δ*psb*O mutant contained ca. 70% the PSII content of wild-type* cells. The mutants listed in Table 2 but not in Table 1 will be described more completely elsewhere (Chu, H.-A. et al., in preparation).

Charge Recombination between Q_A^- and PSII Electron Donors. The kinetics of charge recombination between Q_A^- and the donor side of PSII is sensitive to the presence or absence of photooxidizable Mn ions in PSII (Nixon & Diner, 1990, 1992; Boerner et al., 1992). In *Synechocystis* 6803, the yield of variable chlorophyll fluorescence is believed to be proportional to the concentration of Q_A^- (Philbrick et al., 1991; Nixon et al., 1992b). Consequently, the kinetics of charge recombination can be measured from the decay of fluorescence yield that follows a saturating flash given in the presence of DCMU. Representative data are shown in Figure 2. The decay kinetics were analyzed assuming three exponentially decaying components (fewer components yielded nonrandom residuals). The amplitudes and rates of these components for the mutants discussed in this paper are presented in Table 1. The decay of fluorescence yield in wild-type* cells (Figure 2A) exhibited components of 0.10 s (16%), 0.60 s (43%), and 2.8 s (41%) and reflects charge recombination between Q_A^- and the S_2 state of the Mn cluster (Nixon & Diner, 1990, 1992; Cao et al., 1991; Boerner et al., 1992). The more rapid decay in

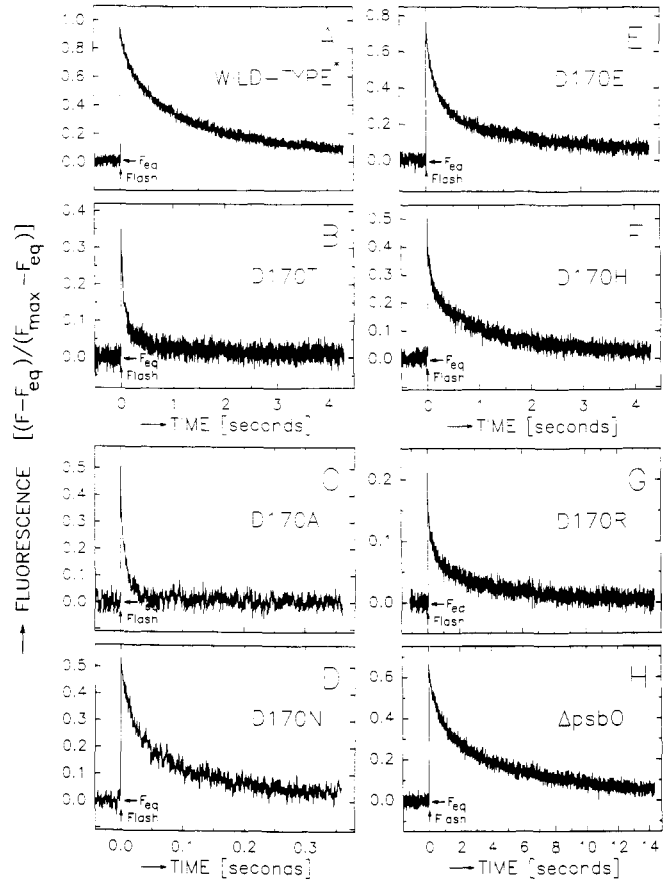

FIGURE 2: Charge recombination kinetics between Q_A^- and oxidized PSII electron donors in wild-type* and mutant cells as measured by the decay of chlorophyll *a* fluorescence yield after a saturating flash given in the presence of DCMU. (A) wild-type*, (B) D170T, (C) D170A, (D) D170N, (E) D170E, (F) D170H, (G) D170R, (H) Δ*psb*O. Note the three different time scales. Conditions: 20 μg of Chl in 0.58 mL of 50 mM MES–NaOH, 25 mM $CaCl_2$, 10 mM NaCl, pH = 6.5, 22 °C. Samples were incubated in darkness for 1 min in the presence of 0.3 mM *p*-benzoquinone and 1 mM potassium ferricyanide before DCMU was added to a concentration of 40 μM (the final concentration of ethanol was 2%). For further details and a definition of F_{eq}, see Materials and Methods. The F_{max} values were obtained by illuminating duplicate samples for 5 s (see Figure 5). The F_{max} values were not increased by the addition of hydroxylamine. Each trace represents the computer average of 8–10 traces. The monitoring flashes were applied at 1.6 kHz.

D170T cells (Figure 2B), with components of 33 ms (67%), 0.27 s (25%), and 4.1 s (6.9%), and in D170A and D170N cells (Figure 2C,D, respectively), reflects charge recombination between Q_A^- and Y_Z^+, as previously demonstrated for cells of D170S, D170A, and D170N (Nixon & Diner, 1990, 1992; Boerner et al., 1992). The charge recombination kinetics in cells of D170E (Figure 2E), D170H (Figure 2F), and D170R (Figure 2G) are markedly heterogeneous, suggesting that a considerable fraction of Q_A^- recombines with Y_Z^+ in these mutants, particularly in D170H and D170R, despite the presence of oxygen-evolving Mn clusters. This heterogeneity will be discussed further below.

The observed rate of charge recombination is determined by the rate of charge recombination between Q_A^- and P_{680}^+ [$\tau_{1/2} \approx 900$ μs in *Synechocystis* 6803 (Metz et al., 1989)] and the equilibrium concentration of P_{680}^+. In reaction centers having an intact, photooxidizable Mn cluster, the concentration of P_{680}^+ is determined by the equilibrium between S_2P_{680} and $S_1P_{680}^+$ (Bouges-Bocquet, 1980; Vass & Styring, 1991; Buser et al., 1992; Buser, 1993). In reaction centers lacking photooxidizable Mn ions, the concentration of P_{680}^+ is

determined by the equilibrium between $Y_Z^+P_{680}$ and $Y_ZP_{680}^+$ (Yerkes et al., 1983; Buser et al., 1990; Buser, 1993). Assuming that the rate of charge recombination between Q_A^- and P_{680}^+ is not affected significantly by the mutation, changes in the observed rate of charge recombination reflect changes in these equilibria, and therefore reflect mutation-induced changes in the midpoint potentials of Y_Z or the Mn cluster. The much slower charge recombination kinetics observed in Δ*psb*O cells (Figure 2H) and in a fraction of reaction centers in D170R cells (Figure 2G) compared to wild-type* cells (Figure 2A) suggests that the midpoint potential of the S_2/S_1 couple has decreased in these mutants. A similar stabilization of the S_2 state has been observed previously in Δ*psb*O mutants from *Synechocystis* (Philbrick et al., 1991; Vass et al., 1992; Burnap et al., 1992) and in spinach PSII membranes that had been depleted of the extrinsic 33-kDa polypeptide (Miyao et al., 1987; Vass et al., 1987a,b). The two slower components of charge recombination in D170E cells (Figure 2E, Table 1) are slightly different than those in wild-type* cells, suggesting that the midpoint potential of the S_2/S_1 couple is slightly altered in the D170E mutant compared to wild-type* cells, as noted previously (Nixon & Diner, 1992; Boerner et al., 1992). In contrast, the slower components in D170H cells (Figure 2F, Table 1) are essentially the same as in wild-type* cells, suggesting that the midpoint potential of the S_2/S_1 couple is relatively unaltered in this mutant. The charge recombination kinetics in D170A cells (Figure 2C) are significantly more rapid than those in D170T and D170N cells (Figure 2B,D, respectively), suggesting that the Y_Z^+/Y_Z midpoint potential is higher in D170A than in the D170T or D170N mutants.

The Fluorescence Yield Induced by a Flash in the Absence and Presence of Hydroxylamine. In all mutants, the increase in fluorescence yield produced by a saturating flash in the absence of hydroxylamine (relative to F_{max}) was significantly lower than in wild-type* cells (Figure 2). Assuming that the rate of charge recombination between Q_A^- and P_{680}^+ is not affected significantly by the mutations, the lower yield could have one or more of three possible causes: (1) significantly slowed electron transfer from Y_Z to P_{680}^+, resulting in a lower quantum yield for the formation of the high fluorescence state $P_{680}Q_A^-$, (2) an increased equilibrium concentration of P_{680}^+ [which quenches chlorophyll *a* fluorescence (Butler, 1972; Butler et al., 1973)] caused by a shift in the equilibrium between $Y_ZP_{680}^+$ and $Y_Z^+P_{680}$ or between $S_1P_{680}^+$ and S_2P_{680}, or (3) the production of a fluorescence quencher other than P_{680}^+ (*e.g.*, Chl^+), presumably by the oxidation of an unidentified species by P_{680}^+.

To test the first possibility, we measured the increase in fluorescence yield produced by the first in a series of saturating flashes given in the presence of hydroxylamine. This compound reduces Y_Z^+ (Bennoun, 1970). By reducing Y_Z^+, hydroxylamine should eliminate the second possibility by driving the equilibrium $Y_Z^+P_{680} \rightleftharpoons Y_ZP_{680}^+$ toward the left. Hydroxylamine should also eliminate the third possibility by keeping potential fluorescence quenchers reduced. At the concentration employed in this study (20 mM), hydroxylamine also extracts the Mn cluster (Cheniae & Martin, 1971). Electron transfer from Y_Z to P_{680}^+ is much slower in the absence of the Mn cluster [20–40 μs (Van Best & Mathis, 1978, Conjeaud et al., 1979)] than in its presence [20–280 ns (Brettel et al., 1984; Meyer et al., 1989)]. Consequently, after extraction of Mn by hydroxylamine, the rate of electron transfer from Y_Z to P_{680}^+ should be the same in all mutants unless this rate is altered by the mutation. Representative

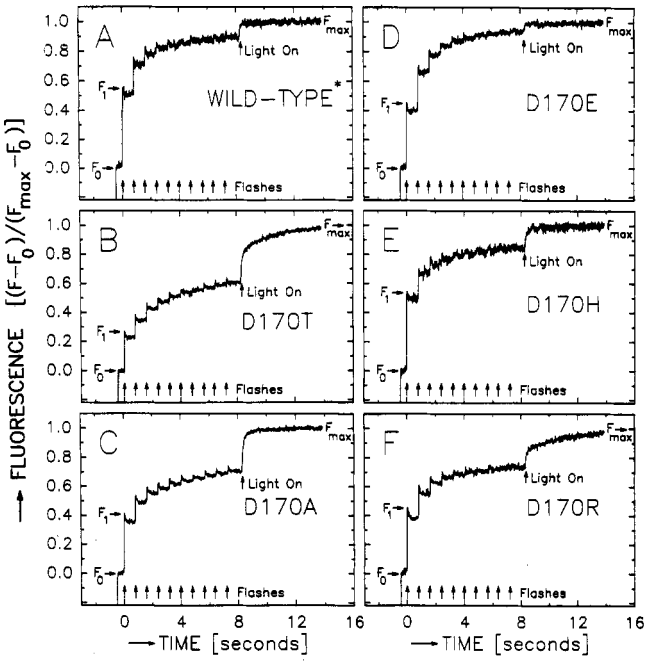

FIGURE 3: Formation of Q_A^- in wild-type* and mutant cells in response to 10 saturating flashes given at 800-ms intervals in the presence of DCMU and hydroxylamine, followed by continuous illumination. (A) Wild-type*, (B) D170T, (C) D170A, (D) D170E, (E) D170H, (F) D170R. The conditions were the same as in Figure 2 except that the cells were incubated in darkness in the presence of *p*-benzoquinone and potassium ferricyanide for 5 min before the addition of DCMU. Hydroxylamine (20 mM) was added 1 min after the DCMU. The monitoring flashes were switched on 2 min after the addition of hydroxylamine, followed 0.5 s later by the saturating flashes (arrows). Continuous illumination (applied to obtain F_{max}) was applied 1.1 s after the 10th flash (arrow). The initial fluorescence yields produced by the monitoring flashes (F_0) are indicated. The monitoring flashes were applied at 1.6 kHz.

data are shown in Figure 3 [because stable F_{eq} levels cannot be achieved in our apparatus in the presence of hydroxylamine, the data are normalized to $(F_{max} - F_0)$ rather than to $(F_{max} - F_{eq})$]. In most of the Asp-170 mutants, the relative fluorescence yield produced by the first flash (F_1) was slightly diminished compared to wild-type* cells. The ratio $(F_1 - F_0)/(F_{max} - F_0)$ was 0.59 ± 0.06 for wild-type* (Figure 3A), 0.31 ± 0.07 for D170T (Figure 3B), 0.43 ± 0.03 for D170A (Figure 3C), 0.48 ± 0.01 for D170E (Figure 3D), 0.57 ± 0.03 for D170H (Figure 3E), 0.46 ± 0.04 for D170R (Figure 3F), and 0.47 ± 0.02 for D170N cells (not shown). The ratio in Δ*psb*O cells (0.78 ± 0.02, not shown), was slightly higher than in wild-type* cells, as reported previously for two other Δ*psb*O strains (Philbrick et al., 1991). Although the $(F - F_0)/(F_{max} - F_0)$ values after 10 flashes were considerably lower in D170T and D170A than in wild-type* cells, these values increased to wild-type* levels (0.91 ± 0.04) when the number of flashes was increased to ca. 100 (not shown).

The lower $(F_1 - F_0)/(F_{max} - F_0)$ ratios in all mutants except D170H compared to wild-type* suggests that electron transfer from Y_Z to P_{680}^+ is slowed in these mutants, and is slowed to the greatest extent in D170T. Slowed electron transfer from Y_Z to P_{680}^+ indicates that most mutations at Asp-170 structurally perturb PSII to some degree. An example of such a perturbation would be a slightly increased distance between Y_Z and P_{680} [*e.g.*, Moser et al. (1992)]. We have no explanation for why these perturbations would be greatest in D170T or be greater in D170E than in D170H. Note that there appears to be no correlation between the relative $(F_1 - F_0)/(F_{max} - F_0)$ ratios (*e.g.*, Figure 3) and the flash-induced fluorescence yields observed in the absence of hydroxylamine

(Figure 2). This lack of correlation indicates that, while slowed electron transfer from Y_Z to P_{680}^+ may *contribute* to the lower flash-induced fluorescence yields observed in the absence of hydroxylamine in some mutants (*e.g.*, D170T), other factors must also be involved.

An indication of whether the lower flash-induced fluorescence yields of Figure 2 are partly caused by an increased equilibrium concentration of P_{680}^+ or by the formation of a fluorescence quencher other than P_{680}^+ can be obtained by examining the kinetics of charge recombination after a flash. If the lower flash-induced yield results from an increased equilibrium concentration of P_{680}^+, the lower yield should correlate with accelerated charge recombination kinetics (Philbrick et al., 1991). Such a correlation may exist for some mutants [*e.g.*, compare D170E (Figure 2E) and D170H (Figure 2F) with wild-type* (Figure 2A)]. However, it clearly does not exist for mutants such as Δ*psb*O and D170R. In these mutants, the flash-induced fluorescence yield in the absence of hydroxylamine is *smaller* than in mutants having more rapid charge recombination kinetics [compare Δ*psb*O (Figure 2H) with wild-type* (Figure 2A) and compare D170R (Figure 2G) with D170A (Figure 2C)]. Consequently, in some mutants [e.g., Δ*psb*O and D170R], the production of an unknown fluorescence quencher must contribute to the lower flash-induced fluorescence yield observed in the absence of hydroxylamine. This conclusion was previously reached for other Δ*psb*O strains by Philbrick et al. (1991).

Quenching of Chlorophyll Fluorescence after the Second and Subsequent Flashes in a Series. The maximum yield of chlorophyll fluorescence produced by each flash in a closely-spaced series given in the absence of DCMU is also sensitive to the presence or absence of photooxidizable Mn ions in PSII (Nixon & Diner, 1990, 1992; Boerner et al., 1992). The highly fluorescent state $Y_Z^+P_{680}Q_A^-$ is formed 20 ns to 40 μs after the first flash, depending on whether or not the Mn cluster is present (see above). The subsequent fluorescence decay represents the oxidation of Q_A^- by Q_B (Bowes & Crofts, 1980). If present, the Mn cluster reduces Y_Z^+ within 30–1300 μs (Dekker et al., 1984b). However, if the Mn cluster is absent or not photooxidizable, Y_Z^+ is reduced by an alternate electron donor (possibly via P_{680}) at a slower rate. If a second saturating flash is given before Y_Z^+ has been reduced (but after Q_A^- has been oxidized by Q_B), the weakly fluorescent state $Y_Z^+P_{680}^+Q_A^-Q_B^-$ is formed. Consequently, the maximum fluorescence yield produced by the second flash will be lower than that produced by the first.

The fluorescence yields produced by each of four flashes given 50 ms apart are shown in Figure 4 for a representative set of mutants. In wild-type* cells (Figure 4A), the maximum fluorescence yield produced by each flash was essentially the same except for small variations attributable to the different S state distribution present before each flash (Delosme, 1972; Zankel, 1973). In contrast, in D170A cells (Figure 4B), the maximum fluorescence yields produced by the second and subsequent flashes were substantially quenched. These data show that the reduction of Y_Z^+ is slowed dramatically in D170A cells (to tens of milliseconds), as expected for a mutant that lacks photooxidizable Mn ions (Nixon & Diner, 1990, 1992; Boerner et al., 1992). Similar data were obtained for the D170N and D170T mutants (not shown).

The rate of electron transfer from Q_A^- to Q_B is multiphasic [*e.g.*, see Cao et al. (1991)]. In all three mutants without photooxidizable Mn ions (D170A, D170N and D170T), the slowest components of this electron transfer step were slower than in wild-type* cells, with significant fractions of Q_A^-

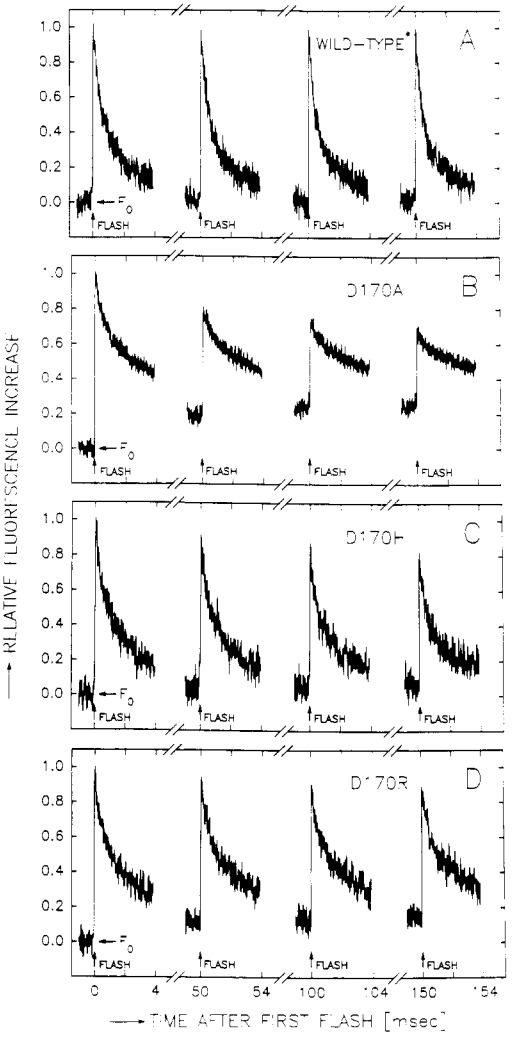

FIGURE 4: Yield of variable chlorophyll *a* fluorescence produced by each of four saturating flashes given at 50-ms intervals to wild-type* and mutant cells. Five milliseconds of data are shown for each flash. (A) Wild-type*, (B) D170A, (C) D170H, (D) D170R. The conditions were the same as in Figure 2 except that cells were incubated in darkness for 1 min (without *p*-benzoquinone or ferricyanide) before the monitoring flashes were switched on, and no DCMU was added. The frequency of the monitoring flashes was switched from 1.6 to 100 kHz for 5 ms beginning 1 ms before each flash. The vertical scales are normalized to the maximum $(F - F_0)/F_0$ values observed after the first flash in each series. These values were 0.46 for A, 0.35 for B, 0.24 for C, and 0.14 for D. Five individual flash series were averaged for B and six for D. Data obtained with cells of D170N and D170T (not shown) resembled that of D170A.

remaining reduced 50 ms after each flash (*e.g.*, compare Figure 4, parts A and B). However, it is not clear if the faster components of electron transfer were also slowed: the fluorescence yield is partially quenched by P_{680}^+ for 100–120 μs following each flash (including the first) in these mutants because electron transfer from Y_Z to P_{680}^+ is slower in the absence of the Mn cluster than in its presence and because the equilibrium concentration of P_{680}^+ is higher (see above).

In many PSII mutants [*e.g.*, D170H (Figure 4C) and D170R (Figure 4D)], the maximum fluorescence yields produced by the second and subsequent flashes were quenched to *intermediate* extents. In addition, the slowest components of electron transfer from Q_A^- to Q_B were slowed to intermediate extents (Figure 4C,D), in proportion to the extent of fluorescence quenching. In many PSII mutants that exhibit intermediate fluorescence quenching and slowed Q_A^- to Q_B electron transfer kinetics, including D170H and D170R, charge recombination after a single flash is markedly

heterogeneous, with Q_A^- recombining with Y_Z^+ in some reaction centers and with the S_2 state in others (see above, Figure 2). There are two reasons why Q_A^- might recombine with Y_Z^+ in some reaction centers and with the S_2 state of the Mn cluster in others. First, electron transfer from Mn to Y_Z^+ may have slowed considerably, allowing Q_A^- to reduce Y_Z^+ in a fraction of reaction centers. Second, a fraction of reaction centers may lack photooxidizable Mn ions *in vivo*. The same reasons can also explain the intermediate extent of fluorescence quenching observed in the same mutants. First, electron transfer from Mn to Y_Z^+ may have slowed considerably, so that, in a fraction of reaction centers, the second flash is applied before Y_Z^+ is reduced. Second, a fraction of reaction centers may lack photooxidizable Mn ion *in vivo*. However, a third explanation for an intermediate extent of fluorescence quenching is that, in some mutants, electron transfer from Y_Z to P_{680}^+ is slowed significantly when the Mn cluster is in its higher oxidation states. This phenomenon has been observed in Ca^{2+}-depleted PSII membranes from spinach (Boussac et al., 1992). If this explanation is correct, the extent of fluorescence quenching observed after the second and subsequent flashes should not depend on the spacing between flashes applied at frequencies greater than 1 Hz: the lifetimes of the S_2 and S_3 states greatly exceed the time between such flashes (Joliot et al., 1971; Forbush et al., 1971). However, in every mutant examined, the extent of quenching diminished as the flash spacing increased, becoming negligible at a flash spacing of 800 ms (not shown). These data show that intermediate quenching arises from slow reduction of Y_Z^+ rather than of P_{680}^+. Consequently, both the intermediate fluorescence quenching and the markedly heterogeneous charge recombination kinetics observed in mutants such as D170H and D170R must be caused by either (1) slow reduction of Y_Z^+ by the Mn cluster or (2) lack of photooxidizable Mn ions in a fraction of PSII reaction centers.

Photoaccumulation of Q_A^-. To determine if a fraction of PSII reaction centers in D170H, D170R, and other mutants lacks bound, photooxidizable Mn ions, cells were illuminated for various times (1–15 s) in the presence of DCMU. After illumination was terminated by a fast shutter, the kinetics of Q_A^- oxidation were analyzed assuming three exponentially decaying components (fewer components yielded nonrandom residuals). The basis for this assay is recent work showing that cytochrome *b*-559 and Y_D are oxidized by P_{680}^+ with low quantum yields (Buser et al., 1990, 1992; Vass & Styring, 1991; Buser, 1993). The rates of oxidation correlate with the equilibrium concentration of P_{680}^+. Consequently, both species are oxidized far more rapidly in Mn-depleted PSII preparations than in intact preparations (Buser et al., 1992; Buser, 1993). Oxidized cytochrome *b*-559 and Y_D^+ are relatively stable species, even in the presence of Q_A^-. During continuous illumination in the presence of DCMU, the states $Y_Z^+Q_A^-$ and $S_2Q_A^-$ form and recombine until the stable states $cyt^{ox}Q_A^-$ and $Y_D^+Q_A^-$ photoaccumulate (Buser et al., 1990, 1992; Buser, 1993). The subsequent oxidation of Q_A^- is a slow process (τ > 1 min). Consequently, if site-directed PSII mutants are illuminated in the presence of DCMU, the stable states $cyt^{ox}Q_A^-$ and $Y_D^+Q_A^-$ should photoaccumulate far more rapidly in reaction centers *without* photooxidizable Mn ions than in reaction centers *with* photooxidizable Mn ions.

Representative data are shown in Figure 5. The decay of fluorescence yield in wild-type* cells after 5 s of illumination (Figure 5A) exhibited components of 0.53 s (56%), 3.0 s (36%), and 1 min (7%). The first two components are similar to the two slower components observed in these cells after a single saturating flash (Figure 2A, Table 1). The amount of the third component increased from 4 to 9% as the illumination time was increased from 1 to 15 s (Figure 6A). The decay of fluorescence yield in D170A cells after 5 s of illumination (Figure 5B) exhibited components of 54 ms (22%), 3.8 s (6%), and 2 min (72%). The amount of the 2-min component increased from 41 to 82% as the illumination time was increased from 1 to 15 s (Figure 6A). The appearance of a 1–2-min component of fluorescence decay in wild-type* and D170A cells after a brief period of continuous illumination is consistent with the photoaccumulation of $cyt^{ox}Q_A^-$ or $Y_D^+Q_A^-$ in a fraction of reaction centers in these strains. We conclude that 7% of the wild-type* and 72% of the D170A reaction centers observable in our measurements photoaccumulated Q_A^- during 5 s of illumination. The vastly different rates of

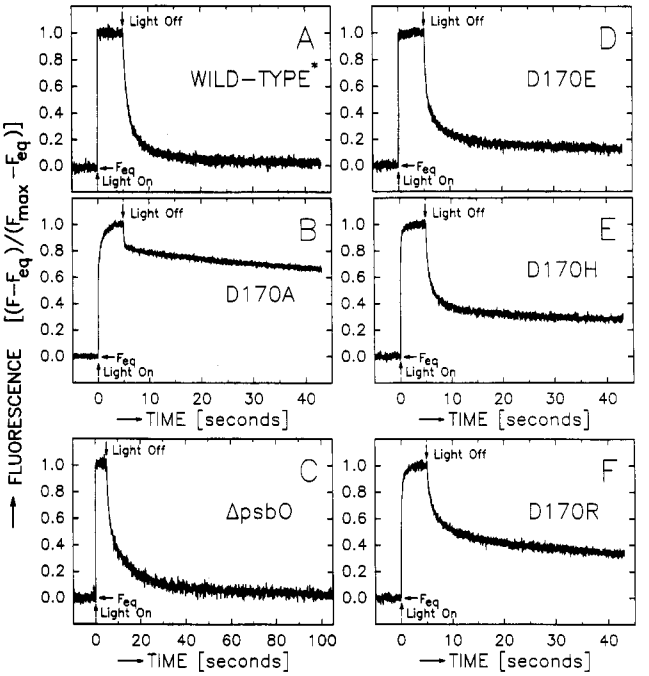

FIGURE 5: Formation and decay of Q_A^- in response to 5 s of continuous illumination in the presence of DCMU: (A) wild-type*, (B) D170A, (C) Δ*psb*O, (D) D170E, (E) D170H, (F) D170R. The conditions were the same as in Figure 2. The onset and termination of illumination (controlled by a shutter that opened in 1.5 ms and closed in 3.0 ms) are indicated by arrows. Note the different time scale for the Δ*psb*0 mutant. For a definition of F_{eq}, see Materials and Methods. The monitoring flashes were applied at 1.6 kHz.

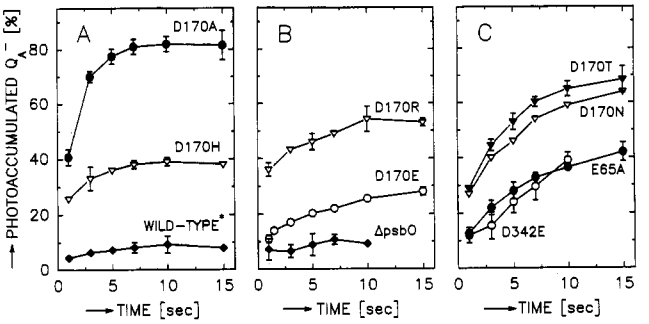

FIGURE 6: The fraction of PSII reaction centers that photoaccumulated Q_A^- after illumination for specific intervals of time. This fraction is defined as that fraction of reaction centers in which Q_A^- is oxidized with a time constant of 1–3 min (see Figure 5 and text). (A) Photoaccumulation of Q_A^- in D170A (top), D170H (middle), and wild-type* (bottom) cells. (B) Photoaccumulation of Q_A^- in D170R (top), D170E (middle), and Δ*psb*O (bottom) cells. (C) Photoaccumulation of Q_A^- in D170T and D170N (top) and in E65A and D342E (bottom) cells. The conditions were the same as in Figure 5.

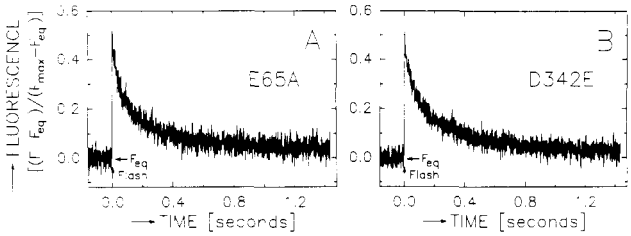

FIGURE 7: Charge recombination kinetics between Q_A^- and oxidized PSII electron donors in (A) E65A and (B) D342E cells. The conditions were the same as in Figure 2. Traces A and B are the computer averages of six and eight traces, respectively. Note that the time scales differ from those in Figure 2. The monitoring flashes were applied at 1.6 kHz.

Q_A^- photoaccumulation in wild-type* and D170A cells (Figure 6A) are consistent with the presence of the Mn cluster in wild-type* cells and its absence in D170A cells.

In mutants that displayed both markedly heterogeneous charge recombination kinetics (Figure 2) and intermediate fluorescence quenching (Figure 4), 20–44% of the fluorescence yield after 5 s of illumination decayed with time constants of 1–3 min [*e.g.*, D170E (Figure 5D), D170H (Figure 5E), and D170R (Figure 5F)] (see Table 1). In these mutants, a significant fraction of reaction centers photoaccumulated Q_A^- during the first second of illumination (Figure 6A,B). The remaining fraction photoaccumulated Q_A^- with a rate similar to that of wild-type* reaction centers. These data imply that significant fractions of reaction centers in D170E, D170H, and D170R cells lack photooxidizable Mn ions. These reaction centers rapidly photoaccumulate Q_A^- during illumination in the presence of DCMU, similarly to D170A reation centers. In these reaction centers, either the high-affinity site from which Mn rapidly reduces Y_Z^+ is devoid of Mn ions or the Mn ion(s) at this site are unable to reduce Y_Z^+.

In the above discussion we have assumed that the observed photoaccumulation of Q_A^- is caused by electron donation from cytochrome *b*-559 or Y_D to P_{680}^+. In principle, however, the photoaccumulation of Q_A^- could be caused by the reduction of Y_Z^+ or the Mn cluster in the charge-separated states $Y_Z^+Q_A^-$ or $S_2Q_A^-$ by electron donors exogenous to PSII, forming the stable states $Y_ZQ_A^-$ or $S_1Q_A^-$. Many compounds reduce the exposed Y_Z^+ radical in Mn-depleted reaction centers far more rapidly than they reduce the protected S_2 state of the Mn cluster in intact reaction centers (Velthuys, 1983; Ghanotakis et al., 1984; Tamura et al., 1986). To determine if the donor(s) responsible for the photoaccumulation of Q_A^- could be exogenous to PSII, we examined the rate of Q_A^- photoaccumulation in the mutants Δ*psb*O, E65A, and D342E (Figure 6B,C). Because Δ*psb*O cells lack the extrinsic 33-kDa polypeptide, Q_A^- should photoaccumulate rapidly in this mutant if the electron donor(s) were exogenous to PSII: the Mn cluster is more accessible to reductants in the absence of the extrinsic 33-kDa polypeptide than in its presence (Tamura & Cheniae, 1985; Tamura et al., 1986, 1990; Burnap & Sherman, 1991; Mei & Yocum, 1993). Indeed, the rapid loss of oxygen evolution in Δ*psb*O cells in darkness (see above) suggests that exogenous reductants capable of reducing the Mn cluster, and, therefore, capable of reducing S_2 to S_1, are present *in vivo*. However, Q_A^- is observed to photoaccumulate very slowly in Δ*psb*O cells (Figure 5C and 6B), at essentially the same rate as in wild-type* cells.

The mutants E65A and D342E are photoautotrophic and evolve oxygen (Table 1). Both mutants exhibit slow charge recombination kinetics (Figure 7A,B) and appear to contain only small fractions of reaction centers that photoaccumulate Q_A^- during the first second of illumination (Figure 6C). Consequently, most reaction centers in these mutants must contain bound, photooxidizable Mn ions. In both mutants, the rates of both Q_A^- photoaccumulation (Figure 6C) and charge recombination (Figure 7A,B) are considerably greater than in wild-type* cells (*cf.*, Figures 2A and 6A, Table 1). The faster charge recombination kinetics observed in E65A and D342E cells implies that the equilibrium concentration of P_{680}^+ is higher in these mutants than in wild-type* cells. Consequently, the rate of Q_A^- photoaccumulation in reaction centers *containing* photooxidizable Mn ions appears to correlate with the equilibrium concentration of P_{680}^+. This correlation also applies to reaction centers that *lack* photooxidizable Mn ions: the rates of both Q_A^- photoaccumulation (Figure 6A,C) and charge recombination (Figure 2B-D) are considerably greater in D170A than in D170N and D170T cells (also see Table 1).

The slow photoaccumulation of Q_A^- in Δ*psb*O cells (Figure 6B) and the correlation of the rate of Q_A^- photoaccumulation with the equilibrium concentration of P_{680}^+ in reaction centers both containing and lacking photooxidizable Mn ions (Figure 6A,C) suggest that, while exogenous reductants may contribute to the photoaccumulation of Q_A^- by reducing Y_Z^+ or the Mn cluster, the dominant reductant must be an intrinsic component of PSII that reduces P_{680}^+ with a low quantum yield.

DISCUSSION

We have described noninvasive procedures for the *in vivo* characterization of mutant PSII complexes that are based on measurements of the yield of chlorophyll *a* fluorescence after a saturating flash in the presence of DCMU, after brief illumination in the presence of DCMU, or after each of a series of saturating flashes in the absence of DCMU. These procedures have been illustrated by their application to mutants from which PSII particles had been previously characterized. Mutants with bound, photooxidizable Mn ions (*e.g.* wild-type* cells) exhibit (1) slow charge recombination kinetics (Figure 2A), (2) no significant quenching of variable fluorescence yield after any flash in a closely-spaced series (Figure 4A), (3) rapid Q_A^- to Q_B electron transfer kinetics (Figure 4A), and (4) slow photoaccumulation of Q_A^- in response to illumination in the presence of DCMU (Figures 5A and 6A). In contrast, mutants that lack photooxidizable Mn ions (*e.g.*, D170A, D170N, and D170T), exhibit (1) rapid charge recombination kinetics (Figure 2B–D), (2) significant quenching of variable fluorescence yield after the second and subsequent flashes in a closely-spaced series (Figure 4B), (3) slowed Q_A^- to Q_B electron transfer kinetics (Figure 4B), and (4) rapid photoaccumulation of Q_A^- in response to illumination in the presence of DCMU (Figures 5B and 6A,C). The vastly different rates of Q_A^- photoaccumulation in mutants containing and lacking photooxidizable Mn ions are consistent with *in vitro* measurements of cytochrome *b*-559 and Y_D photooxidation in Mn-depleted and intact PSII preparations (Buser et al., 1990, 1992; Vass & Styring, 1991; Buser, 1993).

The primary species responsible for the photoaccumulation of Q_A^- is an intrinsic component of PSII. This conclusion is based on the slow photoaccumulation of Q_A^- in Δ*psb*O cells (Figure 6B) and on the correlation between the rate of Q_A^- photoaccumulation and the equilibrium concentration of P_{680}^+ in several mutants containing or lacking photooxidizable Mn ions (Figure 6A,C). It is unlikely that this component is Y_D because Y_D^+ is a very stable species (Babcock & Sauer, 1973) and the cells in our experiments were not extensively dark-

adapted. Consequently, Y_D is probably oxidized in most reaction centers in our samples prior to illumination. A more likely candidate for this component is cytochrome *b*-559 (Buser et al., 1990, 1992; Buser, 1993). Cytochrome *b*-559 reduces P_{680}^+ via a chlorophyll molecule (Thompson & Brudvig, 1988). That at most 80% of reaction centers photoaccumulated Q_A^- in any mutant (Figure 6) may reflect the multiple midpoint potentials associated with this cytochrome (Cramer & Whitmarsh, 1977; Ortega et al., 1988; Thompson et al., 1989). In our experiments, ca. 20% of cytochrome *b*-559 may be in an oxidized form prior to illumination.

It cannot be excluded that other intrinsic components of PSII contribute to the photoaccumulation of Q_A^- in our measurements. Such components include the unidentified species (possibly a histidine residue) whose oxidized form gives rise to the A_T thermoluminescence peak in Mn-depleted PSII membranes [*e.g.*, see the work of Ono and Inoue (1991), Allakhverdiev et al. (1992), and Kramer et al. (1994)] and the tyrosine residue (Boerner & Barry, 1994) that gives rise to the M^+ radical observed in mutants lacking Y_Z or Y_D (Noren & Barry, 1992; Boerner et al., 1993).

Whatever the identity of the reductant responsible for the photoaccumulation of Q_A^-, the markedly heterogeneous rates of photoaccumulation observed in D170H, D170R, and (to a lesser extent) D170E cells (Figure 6A,B) demonstrates that significant fractions of reaction centers in these mutants lack photooxidizable Mn ions *in vivo*. Consistent with this interpretation, D170H and D170R cells exhibit heterogeneous charge recombination kinetics [with significant fractions of Q_A^- recombining with Y_Z^+ (Figure 2F,G)] and intermediate quenching of variable fluorescence yield after the second and subsequent flashes in a closely-spaced series (Figure 4C,D). By comparing the extent of Q_A^- photoaccumulation in D170R, D170H, and D170E cells with that in wild-type* and D170A cells after 10–15 s of illumination (Figure 6A,B), one can estimate that ca. 60% of D170R reaction centers, ca. 40% of D170H reaction centers, and 20–25% of D170E reaction centers lack photooxidizable Mn ions *in vivo*. These estimates are in rough agreement with the fractions of Q_A^- that appear to recombine with Y_Z^+ after a single saturating flash (Figure 2, Table 1). However, for several reasons, these estimates should be considered to be very approximate. First, because our fluorescence monitoring flashes exert an actinic effect on the measured samples, a fraction of reaction centers having long charge recombination halftimes would have escaped detection in our measurements (Boerner et al., 1992). This fraction was ca. 25% in wild-type* and D170E cells, ca. 11% in D170H and D170R cells, and ca. 5% in D170A, D170T, and D170N cells (see the discussion of F_{eq} values in Materials and Methods). Second, the observed rates of Q_A^- photoaccumulation differed considerably between mutants containing similar fractions of reaction centers with photooxidizable Mn ions. The observed rate depended on the equilibrium concentrations of P_{680}^+ in these mutants (*e.g.*, Figure 6A,C). Third, the multiphasic nature of charge recombination rates in PSII [*e.g.*, see the work of Joliot (1974) and Gerken et al. (1989); also see Table 1] complicates attempts to assign specific recombination processes to specific rates. For example, quantitative analyses of charge recombination kinetics required three exponentially decaying components in all mutants, including wild-type* cells. It is unlikely that 16% of Q_A^- recombines with Y_Z^+ in wild-type* cells (Table 1).

In spite of the quantitation difficulties, the fact that significant fractions of reaction centers in D170H, D170R, and (to a lesser extent) D170E cells rapidly photoaccumulate Q_A^- when illuminated in the presence of DCMU demonstrates that significant fractions of reaction centers in these mutants lack photooxidizable Mn ions *in vivo*. In these fractions of reaction centers, either the high-affinity site from which Mn ions rapidly reduce Y_Z^+ is devoid of Mn ions or the Mn ion(s) bound at this site are unable to reduce Y_Z^+.

That significant fractions of PSII reaction centers in mutants such as D170H and D170R lack photooxidizable Mn ions implies that, in these mutants, the Mn cluster is unstable or is assembled inefficiently. In support of this conclusion, the fluorescence properties of wild-type *Synechocystis* cells propagated in media lacking Cl^- ions resemble those of D170H or D170E cells, depending on the culture examined: Between 13% and 50% of the reaction centers in these cells lack photooxidizable Mn ions *in vivo* (Chu et al., in preparation). The Mn cluster is assembled inefficiently in the presence of low concentrations of Cl^- ions *in vitro* (Miyao & Inoue, 1991) and is unstable in the *absence* of Cl^- ions *in vitro* (Lindberg et al., 1993).

The assembly and activation of the Mn cluster *in vivo* is a low quantum yield process that involves (1) photooxidation of a bound Mn^{2+} ion to form an unstable Mn^{3+} intermediate, (2) ligation of a second Mn^{2+}ion to form an unstable binuclear Mn^{2+}–Mn^{3+} intermediate, (3) photooxidation of the second Mn^{2+} ion to form a relatively stable binuclear Mn^{3+}–Mn^{3+} complex, and (4) ligation of two further Mn^{2+} ions (Tamura & Cheniae, 1987, 1988; Ono and Inoue, 1987; Miller & Brudvig, 1989, 1990). Conformational changes in PSII are believed to precede the ligation of the second Mn^{2+} ion (Tamura & Cheniae, 1987, 1988; Ono & Inoue, 1987; Miyao & Inoue, 1991). In mutants, the efficiency of the assembly process would presumably diminish if a ligand to one of the Mn ions was lost or if structural changes associated with the mutation further destabilized the Mn^{3+} or binuclear Mn^{2+}–Mn^{3+} intermediates or interfered with the putative conformational changes that precede the ligation of the second Mn^{2+} ion. Alterations to these conformational changes could also destabilize the binuclear Mn^{3+}–Mn^{3+} complex and/or the fully assembled cluster. Under such circumstances, the loss of one Mn ion may lead rapidly to the loss of the entire Mn cluster.

As noted earlier, the slowest components of electron transfer from Q_A^- to Q_B are slowed in mutants that lack photooxidizable Mn ions (*e.g.*, D170A, Figure 4B). Furthermore, the slowest components slowed in proportion to the extent of fluorescence quenching observed after the second and subsequent flashes in a series [*e.g.*, D170H and D170R (Figure 4C,D)]. Treatments that alter the donor side of PSII (*e.g.*, removal of extrinsic polypeptides or the Mn cluster) have been shown to slow electron transfer from Q_A^- to Q_B (Dekker et al., 1984a), alter the equilibrium between $Q_A^-Q_B$ and $Q_AQ_B^-$ (van Gorkom et al., 1982), and abolish the ability of Q_B to function as a two-electron accumulator (Wensink et al., 1984; Dekker et al., 1984a). Perhaps the conformational changes that are believed to precede the ligation of the second Mn^{2+} ion during assembly of the Mn cluster *in vivo* accelerate electron transfer from Q_A^- to Q_B. If so, the intermediate Q_A^- to Q_B electron transfer rates observed in mutants with intermediate fluorescence quenching (*e.g.*, D170H and D170R) would be consistent with a fraction of reaction centers in these mutants lacking even partially assembled Mn clusters. Conversely, reaction centers in non-oxygen-evolving, non-photoautotrophic mutants that exhibit relatively normal Q_A^- to Q_B electron transfer kinetics (Chu et al., in preparation) may contain Mn clusters that are at least partly assembled, but that have

significantly altered redox properties.

The *in vivo* characterization procedures described in this manuscript are easily applied to mutants that evolve little or no oxygen and will facilitate the study of PSII mutants that have labile oxygen-evolving complexes. By characterizing mutant PSII complexes by noninvasive methods *in vivo*, possible isolation-induced artifacts are avoided. The information obtained permits PSII isolation efforts to be concentrated on mutants with the stablest Mn clusters, permits the extent of isolation-induced alterations to be determined, and guides systematic spectroscopic studies of isolated PSII particles to mutants of particular interest.

ACKNOWLEDGMENT

We would like to thank G. T. Babcock, B. A. Barry, T. M. Bricker, R. L. Burnap, B. A. Diner, D. F. Ghanotakis, P. J. Nixon, and C. F. Yocum for many fruitful discussions. We are particularly indebted to P. J. Nixon and B. A. Diner for sharing the results of their parallel site-directed-mutagenesis studies prior to publication, to R. L. Burnap for the gift of the Δ*psb*O strain, to W. F. J. Vermaas for the gift of [^{14}C]DCMU and for advice concerning its use, to L. M. Kienitz for help modifying the fluorometer and for building the timing and flashlamp circuitry, and to B. A. Barry, B. A. Diner, H. Kless, W. F. J. Vermaas, C. F. Yocum, and the reviewers for helpful comments on the original manuscript.

REFERENCES

Allakhverdiev, S. I., Klimov, V. V., & Demeter, S. (1992) *FEBS Lett. 297*, 51–54.

Andersson, B., & Styring, S. (1991) *Curr. Top. Bioenerget. 16*, 1–81.

Babcock, G. T., & Sauer, K. (1973) *Biochim. Biophys. Acta 325*, 483–503.

Bennoun, P. (1970) *Biochim. Biophys. Acta 216*, 357–363.

Boerner, R. J., & Barry, B. A. (1994) *J. Biol. Chem. 269*, 134–137.

Boerner, R. J., Nguyen, A. P., Barry, B. A., & Debus, R. J. (1992) *Biochemistry 31*, 6660–6672.

Boerner, R. J., Bixby, K. A., Nguyen, A. P., Noren, G. H., Debus, R. J., & Barry, B. A. (1993) *J. Biol. Chem. 268*, 1817–1823.

Bouges-Bocquet, B. (1980) *Biochim. Biophys. Acta 594*, 85–103.

Boussac, A., Sétif, P., & Rutherford, A. W. (1992) *Biochemistry 31*, 1224–1234.

Bowes, J. M., & Crofts, A. R. (1980) *Biochim. Biophys. Acta 590*, 373–384.

Brettel, K., Schlodder, E., & Witt, H. T. (1984) *Biochim. Biophys. Acta 766*, 403–415.

Brudvig, G. W., & Crabtree, R. H. (1989) *Prog. Inorg. Chem. 37*, 99–142.

Burnap, R. L., & Sherman, L. A. (1991) *Biochemistry 30*, 440–446.

Burnap, R. L., Shen, J.-R., Jursinic, P. A., Inoue, Y., & Sherman, L. A. (1992) *Biochemistry 31*, 7404–7410.

Buser, C. A. (1993) Ph.D. Dissertation, Yale University.

Buser, C. A., Thompson, L. K., Diner, B. A., & Brudvig, G. W. (1990) *Biochemistry 29*, 8977–8985.

Buser, C. A., Diner, B. A., & Brudvig, G. W. (1992) *Biochemistry 31*, 11449–11459.

Butler, W. L. (1972) *Proc. Natl. Acad. Sci. U.S.A. 69*, 3420–3422.

Butler, W. L., Visser, J. W. M., & Simons, H. L. (1973) *Biochim. Biophys. Acta 292*, 140–151.

Cao, J., Vermaas, W. F. J., & Govindjee (1991) *Biochim. Biophys. Acta 1059*, 171–180.

Cheniae, G. M., & Martin, I. F. (1971) *Plant Physiol. 47*, 568–575.

Chisholm, D. A. (1989) *Cyanonews 6*, 3.

Conjeaud, H., Mathis, P., & Paillotin, G. (1979) *Biochim. Biophys. Acta 546*, 280–291.

Cornish-Bowden, A. (1979) *Fundamentals of Enzyme Kinetics*, Butterworths, London.

Cramer, W. A., & Whitmarsh, J. (1977) *Annu. Rev. Plant Physiol. 28*, 133–172.

Debus, R. J., Barry, B. A., Sithole, I., Babcock, G. T., & McIntosh, L. (1988) *Biochemistry 27*, 9071–9074.

Debus, R. J., Nguyen, A. P., & Conway, A. B. (1990) in *Current Research in Photosynthesis* (Baltscheffsky, M., Ed.) Vol. I, pp 829–832, Kluwer Academic Publishers, Dordrecht.

Debus, R. J. (1992) *Biochim. Biophys. Acta 1102*, 269–352.

Dekker, J. P., Ghanotakis, D. F., Plijter, J. J., van Gorkom, H. J., & Babcock, G. T. (1984a) *Biochim. Biophys. Acta 767*, 515–523.

Dekker, J. P., Plijter, J. J., Ouwehand, L., & van Gorkom, H. J. (1984b) *Biochim. Biophys. Acta 767*, 176–179.

Delosme, R. (1972) in *Proceedings of the Second International Congress on Photosynthesis Research* (Forti, G., Avron, M., & Melandri, A., Eds.) Vol. I, pp 187–195, Dr. W. Junk N. V. Publishers, The Hague.

Diner, B. A., & Nixon, P. J. (1992) *Biochim. Biophys. Acta 1101*, 134–138.

Diner, B. A., Nixon, P. J., & Farchaus, J. W. (1991) *Curr. Opin. Struct. Biol. 1*, 546–554.

DuBose, R. F., & Hartl, D. L. (1990) *BioTechniques 8*, 271–274.

Duysens, L. N. M., & Sweers, H. E. (1963) in *Studies on Microalgae and Photosynthtic Bacteria* (Miyachi, S., Ed.) pp 353–372, University of Tokyo Press, Tokyo.

Eisenthal, R., & Cornish-Bowden, A. (1974) *Biochem. J. 139*, 715–720.

Forbush, B., Kok, B., & McGloin, M. P. (1971) *Photochem. Photobiol. 14*, 307–321.

Gerken, S., Dekker, J. P., Schlodder, E., & Witt, H. T. (1989) *Biochim. Biophys. Acta 977*, 52–61.

Ghanotakis, D. F., Babcock, G. T., & Yocum, C. F. (1984) *Biochim. Biophys. Acta 765*, 388–398.

Holzwarth, A. R. (1991) in *Chlorophylls* (Scheer, H., Ed.) pp 1125–1151, CRC Press, Boca Raton.

Holzwarth, A. R., & Roelofs, T. A. (1992) *J. Photochem. Photobiol. B.: Biol., 15*, 45–62.

Ikeuchi, M. (1992) *Bot. Mag. Tokyo 105*, 327–373.

Joliot, A. (1974) *Biochim. Biophys. Acta 357*, 439–448.

Joliot, P., Joliot, A., Bouges, B., & Barbieri, G. (1971) *Photochem. Photobiol. 14*, 287–305.

Kirilovsky, D. L., Boussac, A. G. P., van Mieghem, F. J. E., Ducruet, J.-M. R. C., Sétif, P. R., Yu, J., Vermaas, W. F. J., & Rutherford, A. W. (1992) *Biochemistry 31*, 2099–2107.

Kramer, D. M., Roffey, R. A., Govindjee, & Sayre, R. T. (1994) *Biochim. Biophys. Acta* (in press).

Krause, G. H., & Weis, E. (1991) *Annu. Rev. Plant Physiol. Plant Mol. Biol. 42*, 313–349.

Kusukawa, N., Uemori, T., Asada, K., & Kato, I. (1990) *BioTechniques 9*, 66–72.

Leibl, W., Breton, J., Deprez, J., & Trissl, H.-W. (1989) *Photosynth. Res. 22*, 257–275.

Lichtenthaler, H. K. (1987) *Methods Enzymol. 148*, 350–382.

Lindberg, K., Vänngård, T., & Andréasson, B. (1993) *Photosynth. Res. 38*, 401–408.

Mayes, S. R., Cook, K. M., Self, S. J., Zhang, Z., & Barber, J. (1991) *Biochim. Biophys. Acta 1060*, 1–12.

Mei, R., & Yocum, C. F. (1993) *Photosynth. Res. 38*, 449–453.

Metz, J. G., Nixon, P. J., Rögner, M., Brudvig, G. W., & Diner, B. A. (1989) *Biochemistry 28*, 6960–6969.

Meyer, B., Schlodder, E., Dekker, J. P., & Witt, H. T. (1989) *Biochim. Biophys. Acta 974*, 36–43.

Miller, A.-F., & Brudvig, G. W. (1989) *Biochemistry 28*, 8181–8190.

Miller, A.-F., & Brudvig, G. W. (1990) *Biochemistry 29*, 1385–1392.

Miyao, M., & Inoue, Y. (1991) *Biochemistry 30*, 5379–5387.
Miyao, M., Murata, N., Lavorel, J., Maison-Peteri, B., Boussac, A., & Étienne, A.-L. (1987) *Biochem. Biophys. Acta 890*, 151–159.
Moser, C. C., Keske, J. M., Warncke, K., Farid, R. S., & Dutton, P. L. (1992) *Nature 355*, 796–802.
Nixon, P. J., & Diner, B. A. (1990) in *Proceedings of the Twelfth Annual International Conference of the IEEE Engineering in Medicine and Biology Society* (Pedersen, P. C., & Onarai, B., Eds.) pp 1732–1734, IEEE, New York.
Nixon, P. J., & Diner, B. A. (1992) *Biochemistry 31*, 942–948.
Nixon, P. J., Chisholm, D. A., & Diner, B. A. (1992a) in *Plant Protein Engineering* (Shewry, P., & Gutteridge, S., Eds.) pp 93–141, Cambridge University Press, Cambridge.
Nixon, P. J., Trost, J. T., & Diner, B. A. (1992b) *Biochemistry 31*, 10859–10871.
Noren, G. H., & Barry, B. A. (1992) *Biochemistry 31*, 3335–3342.
Noren, G. H., Boerner, R. J., & Barry, B. A. (1991a) *Biochemistry 30*, 3943–3950.
Noren, G. H., Boerner, R. J., Bixby, K. A., & Barry, B. A. (1991b) *Biophys. J. 59*, 145a.
Ono, T.-A., & Inoue, Y. (1987) *Plant Cell Physiol. 28*, 1293–1299.
Ono, T.-A., & Inoue, Y. (1991) *FEBS Lett. 278*, 183–186.
Ortega, J. M., Hervás, M., & Losada, M. (1988) *Eur. J. Biochem. 171*, 449–455.
Pecoraro, V. L. (1988) *Photochem. Photobiol. 48*, 249–264.
Philbrick, J. B., Diner, B. A., & Zilinskas, B. A. (1991) *J. Biol. Chem. 266*, 13370–13376.
Porter, W. R., & Trager, W. F. (1977) *Biochem. J. 161*, 293–302.
Putnam-Evans, C., & Bricker, T. M. (1992) *Biochemistry 31*, 11482–11488.
Renger, G. (1993) *Photosynth. Res. 38*, 229–247.
Rippka, R., Deruelles, J., Waterbury, J. B., Herdman, M., & Stanier, R. Y. (1979) *J. Gen. Microbiol. 111*, 1–61.
Roelofs, T. A., Lee, C.-H., & Holzwarth, A. R. (1992) *Biophys. J. 61*, 1147–1163.
Rutherford, A. W., Zimmermann, J.-L., & Boussac, A. (1992) in *The Photosystems: Structure, Function and Molecular Biology* (Barber, J., Ed.) pp 179–229, Elsevier Science Publishers, B. V., Amsterdam.
Schatz, G. H., Brock, H., & Holzwarth, A. R. (1988) *Biophys. J. 54*, 397–405.
Schreiber, U. (1986) *Photosynth. Res. 9*, 261–272.
Svensson, B., Vass, I., & Styring, S. (1991) *Z. Naturforsch, 46c*, 765–776.
Tamura, N., & Cheniae, G. M. (1985) *Biochim. Biophys. Acta 809*, 245–259.
Tamura, N., & Cheniae, G. M. (1987) *Biochim. Biophys. Acta 890*, 179–194.
Tamura, N., & Cheniae, G. M. (1988) in *Light-Energy Transduction in Photosynthesis: Higher Plant and Bacterial Models* (Stevens, S. E., Jr., & Bryant, D. A., Eds.) pp 227–242, American Society of Plant Physiologists, Rockville, MD.
Tamura, N., Radmer, R., Lantz, S., Cammarata, K. V., & Cheniae, G. M. (1986) *Biochim. Biophys. Acta 850*, 369–379.
Tamura, N., Inoué, H., & Inoue, Y. (1990) *Plant Cell Physiol. 31*, 469–477.
Thompson, L. K., & Brudvig, G. W. (1988) *Biochemistry 27*, 6653–6658.
Thompson, L. K., Miller, A.-F., Buser, C. A., de Paula, J. C., & Brudvig, G. W. (1989) *Biochemistry 28*, 8048–8056.
Van Best, J. A., & Mathis, P. (1978) *Biochim. Biophys. Acta 503*, 178–188.
van Gorkom, H. J., Thielen, A. P. G. M., & Gorren, A. C. F. (1982) in *Function of Quinones in Energy Conserving Systems* (Trumpower, B. L., Ed.) pp 213–225, Academic Press, New York.
Vass, I., & Styring, S. (1991) *Biochemistry 30*, 830–839.
Vass, I., Ono, T.-A., & Inoue, Y. (1987a) *FEBS Lett. 211*, 215–220.
Vass, I., Ono, T.-A., & Inoue, Y. (1987b) *Biochim. Biophys. Acta 892*, 224–235.
Vass, I., Cook, K. M., Deák, Zs., Mayes, S. R., & Barber, J. (1992) *Biochim. Biophys. Acta 1102*, 195–201.
Velthuys, B. R. (1983) in *The Oxygen Evolving System of Photosynthesis* (Inoue, Y., Crofts, A. R., Govindjee, Murata, N., Renger, G., & Satoh, Ki., Eds.) pp 83–90, Academic Press, Tokyo.
Vermaas, W. F. J., Charité, J., & Shen, G. (1990) *Z. Naturforsch. 45c*, 359–365.
Vermaas, W. F., J., Styring, S., Schröder, W. P., & Andersson, B. (1993) *Photosynth. Res. 38*, 249–263.
Wensink, J., Dekker, J. P., & van Gorkom, H. J. (1984) *Biochim. Biophys. Acta 765*, 147–155.
Whitelegge, J. P., Koo, D., & Erickson, J. M. (1992) in *Research in Photosynthesis* (Murata, N., Ed.) Vol. II, pp 151–154, Kluwer Academic Publishers, Dordrecht.
Williams, J. G. K. (1988) *Methods Enzymol. 167*, 766–778.
Wollman, F.-A. (1978) *Biochim. Biophys. Acta 503*, 263–273.
Yerkes, C. T., Babcock, G. T., & Crofts, A. R. (1983) *FEBS Lett. 158*, 359–363.
Zankel, K. L. (1973) *Biochim. Biophys. Acta 325*, 138–148.